

Drivers of the severity of the extreme hot summer of 2015 in western China

Article

Accepted Version

Chen, W. and Dong, B. ORCID: <https://orcid.org/0000-0003-0809-7911> (2018) Drivers of the severity of the extreme hot summer of 2015 in western China. *Journal of Meteorological Research*, 32 (6). pp. 1002-1010. ISSN 2198-0934 doi: <https://doi.org/10.1007/s13351-018-8004-y> Available at <https://centaur.reading.ac.uk/79536/>

It is advisable to refer to the publisher's version if you intend to cite from the work. See [Guidance on citing](#).

To link to this article DOI: <http://dx.doi.org/10.1007/s13351-018-8004-y>

Publisher: Springer

All outputs in CentAUR are protected by Intellectual Property Rights law, including copyright law. Copyright and IPR is retained by the creators or other copyright holders. Terms and conditions for use of this material are defined in the [End User Agreement](#).

www.reading.ac.uk/centaur

CentAUR

Central Archive at the University of Reading

Reading's research outputs online



1 Citation: Chen, W., B. Dong., 2018: Drivers of the extreme hot summer of 2015 in
2 western China. *J. Meteor. Res.*, **32**(6), doi: 10.1007/s13351-018-8004-y.(in
3 press)

5 **Drivers of the Severity of the Extreme Hot** 6 **Summer of 2015 in Western China**

7
8 Wei CHEN^{1*} and Buwen DONG

9 *1 LASG, Institute of Atmospheric Physics, Chinese Academy of Sciences, Beijing 100029, China*

10 *2 National Centre for Atmospheric Science–Climate, Department of Meteorology, University of*
11 *Reading, Reading RG6 6AH, UK*

12
13
14
15
16
17 (Received January 15, 2018; in final form August 28, 2018)

18
19
20
21
22
23 Supported by the National Natural Science Foundation of China (416750788,
24 U1502233, 41320104007), the Youth Innovation Promotion Association of CAS
25 (2018102), and the Natural Environment Research Council via the National Centre
26 for Atmospheric Science

27
28
29 Corresponding author: chenwei@mail.iap.ac.cn.

30 ©The Chinese Meteorological Society and Springer-Verlag Berlin Heidelberg 2018

31

ABSTRACT

32

33 Western China experienced an extreme hot summer in 2015, breaking a number
34 of temperature records. The summer mean surface air temperature (SAT) anomaly
35 was twice the interannual variability. The hottest daytime temperature (T_{Xx}) and
36 warmest night-time temperature (T_{Nx}) were the highest in China since 1964. This
37 extreme hot summer occurred in the context of steadily increasing temperatures in
38 recent decades. We carried out a set of experiments to evaluate the extent to which the
39 changes in sea surface temperature (SST)/sea ice extent (SIE) and anthropogenic
40 forcing drove the severity of the extreme summer of 2015 in western China. Our
41 results indicate that about 65–72% of the observed changes in the seasonal mean SAT
42 and the daily maximum (T_{max}) and daily minimum (T_{min}) temperatures over western
43 China resulted from changes in boundary forcings, including the SST/SIE and
44 anthropogenic forcing. For the relative role of individual forcing, the direct impact of
45 changes in anthropogenic forcing explain about 42% of the SAT warming and 60%
46 (40%) of the increase in T_{Nx} and T_{min} (T_{Xx} and T_{max}) in the model response. The
47 changes in SST/SIE contributed to the remaining surface warming and the increase in
48 hot extremes, which are mainly the result of changes in the SST over the Pacific
49 Ocean, where a super El Niño event occurred. Our study indicates a prominent role
50 for the direct impact of anthropogenic forcing in the severity of the extreme hot
51 summer in western China in 2015, although the changes in SST/SIE, as well as the
52 internal variability of the atmosphere, also made a contribution.

53 Keywords: severity of temperature extremes, summer 2015, western China,
54 anthropogenic forcing

55

56

57

58 **1. Introduction**

59 2015 was the hottest year globally in terms of the surface air temperature (SAT)
60 since modern meteorological records began ([WMO Press Conference, 25 November](#)
61 [2015](#)). The SAT in China during 2015 broke all historical records and was the
62 warmest year since the complete weather record has appeared ([CMA, 2016](#)). In
63 particular, compared to the same period in history, the SAT and extreme temperature
64 records were both broken over western China in summer (June, July and August)
65 2015. Some observational stations in Xinjiang and Yunnan provinces recorded
66 historical extremes for the daily maximum temperature and the number of extreme hot
67 days ([CMA, 2016](#)). Turpan station experienced its highest recorded maximum
68 temperature of 47.5 °C on 24 July 2015, which occurred after nine consecutive hot
69 days with maximum temperatures >45 °C from 16 July 2015 ([Xinhua net, 24 July](#)
70 [2015](#)).

71 The global increase in hot extremes is attributed to anthropogenic activity
72 ([Christidis et al., 2011](#); [Seneviratne et al., 2012](#); [Bindoff et al., 2013](#); [King et al., 2015](#),
73 [2016](#)). On the regional scale, the combined influence of anthropogenic forcing and
74 natural atmospheric variability can be detected in temperature extremes over many
75 land areas ([Zwiers et al., 2011](#); [Zhou et al., 2016](#)). Changes in anthropogenic forcing
76 and sea surface temperatures (SSTs) explain two-thirds of the magnitude of the 2015
77 heatwave over central Europe ([Dong et al., 2016a](#)). Anthropogenic activities doubled
78 the probability of the 2013 heatwave in central and eastern China ([Ma et al., 2017](#)).

79 An attribution study may help our understanding of how much anthropogenic
80 climate change has contributed to the change in the risk (probability) or severity
81 (magnitude) of observed events (e.g. [Otto et al., 2012](#); [Stott et al., 2013](#); [Stott, 2016](#)).

82 It is possible to estimate how factors such as anthropogenic activity modify the risk
83 and contribute to the severity of events, although a specific extreme event cannot be
84 attributed to a single reason. One extreme event can be considered ‘mostly natural’ in
85 terms of the severity and ‘mostly anthropogenic’ in terms of the risk of occurrence,
86 such as the 2010 Russian heatwave (e.g. [Dole et al., 2011](#); [Rahmstorf and Coumou,](#)
87 [2011](#)). These are two complementary aspects of an event and are not mutually
88 exclusive, but depend on what question is being asked in addressing the attribution of
89 individual weather events to external drivers of climate.

90 Previous studies have attributed human influence to the risk of the extreme heat
91 event over western China in 2015 ([Miao et al., 2016](#); [Sun et al., 2016](#)). Such an
92 extreme event can be increased three-fold due to anthropogenic influences ([Miao et](#)
93 [al., 2016](#)). [Sun et al. \(2016\)](#) further confirmed that there was more than 90% chance
94 for this increase to be at least three-and-a-half-fold. These studies focused on the risk
95 of this kind of event, but ignored the severity of such extreme events. Severity is a
96 crucial features of extreme hot events and is directly related to an increase in mortality
97 ([Kilbourne, 1997](#); [D áz et al. 2002](#)). As a semi-arid region, western China has a
98 shortage of water resources and extreme heat events may result in ecological crises.

99 We performed a set of numerical experiments to assess the extent to which

100 changes in the SST/sea ice extent (SIE) and anthropogenic forcing drove the severity
101 of the extreme hot summer in western China in 2015 and to quantify the relative roles
102 of individual forcing factors. The structure of the paper is as follows. Section 2
103 describes the data and design of the model experiment. The observed changes over
104 western China in summer 2015 are discussed in Section 3. Section 4 presents the
105 simulated changes in response to different forcings and quantitatively evaluates the
106 relative role of individual forcings in the severity of the extreme hot summer in
107 western China in 2015. The conclusion and discussion are presented in Section 5.

108 **2. Data and methods**

109 The observational data were extracted from records of the national climatological
110 daily temperature from 1964 to 2015 at 165 stations in western China (west of 105 °
111 E). These station observations are reliable and are representative of the region because
112 the warming signals and extreme hot events are on a large spatial scale, although the
113 station density is poor in some areas. In addition to the observed summer mean SAT,
114 some extreme temperatures indices, including T_{\max} (the daily maximum temperature),
115 T_{\min} (the daily minimum temperature), the diurnal temperature range (DTR), T_{Xx} (the
116 annual hottest daytime temperature) and T_{Nx} (the annual warmest night-time
117 temperature) were obtained. Each index was calculated for each individual station and
118 then the regional mean was calculated.

119 An atmospheric configuration of the Meteorological Office Hadley Centre Global
120 Environment Model version 3 (HadGEM3-A) was used in this study (Hewitt et al.,

2011). This model has a horizontal resolution of 1.875 ° longitude by 1.25 ° latitude and 85 vertical levels. We performed a set of experiments to detect the relative contribution of changes in the SST/SIE and forcing by anthropogenic greenhouse gases (GHG) and anthropogenic aerosols (AA) over western China in the extreme hot summer of 2015. Each experiment had 25 ensemble members and we analysed the ensemble mean. The CONTROL experiment was performed for the period 1964–1993. Four other experiments (2015ALL, 2015SST, 2015SSTGHG and 2015SSTATL) were performed for the period November 2014 to October 2015 with different forcings (Table 1).

There were two preconditions in this study: (1) we assumed that the responses to different forcings were added linearly and (2) we considered the changes in the SST/SIE and anthropogenic forcing as independent factors. The influence of individual forcing components on the temperatures in summer 2015 was examined. These components included: all forcing (2015All–CONTROL), GHG and anthropogenic aerosols (2015All–2015SST), GHG only (2015SSTGHG–2015SST), anthropogenic aerosols only (2015All–2015SSTGHG), global SSTs (2015SST–CONTROL), Pacific SSTs only (2015SST–2015SSTATL) and Atlantic SSTs only (2015SSTATL–CONTROL). The same set of experiments was used in the attribute study of the 2015 summer European heatwave (Dong et al., 2016a).

Table 1. Summary of numerical experiments.

Experiment	Boundary conditions
CONTROL	Forced with monthly mean climatological SSTs and SIE averaged over

	the period 1964–1993 using HadISST data (Rayner et al., 2003) and with anthropogenic greenhouse gas (GHG) concentrations averaged over the same period and anthropogenic aerosol (AA) emissions averaged over the period 1970–1993 (Lamarque et al., 2010)
2015ALL	Forced with monthly mean SSTs and SIE from November 2014 to October 2015 using HadISST data, with the GHG concentrations in 2014 (WMO 2015) and AA emissions for 2015 from RCP4.5 scenario (Lamarque et al., 2011)
2015SSTGHG	As 2015ALL, but with AA emissions the same as in the CONTROL experiment
2015SST	As 2015ALL, but with GHG concentrations and AA emissions the same as in the CONTROL experiment
2015SSTATL	As 2015SST, but with SSTs outside the Atlantic the same as in the CONTROL experiment

141 SIE, sea ice extent; SST, sea surface temperature.

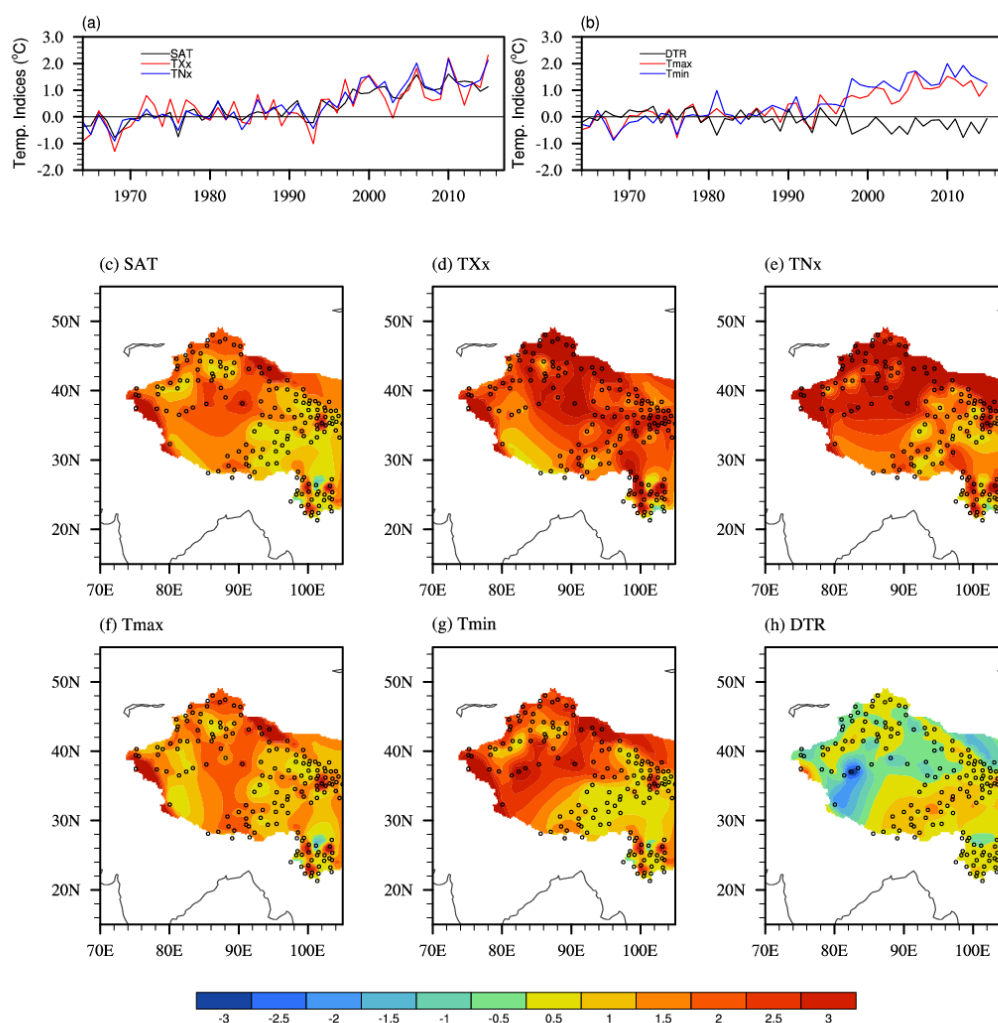
142 **3. Observed changes over western China during summer**

143 **2015**

144 Figure 1a and 1b show the temporal evolution of the SAT and extreme
 145 temperature anomalies averaged over western China relative to the climatological
 146 average from 1964 to 1993. The SAT anomaly over western China in summer 2015
 147 was 1.13 °C, twice the interannual variability of the SAT anomaly (0.60 °C). The SAT
 148 warming in 2015 occurred in the context of steadily increasing temperatures in recent
 149 decades, with a linear trend of 0.34 °C/decade. Summer 2015 set the highest records
 150 for the temperature extremes T_{Xx} and T_{Nx} since 1964. The anomalous T_{Xx} and T_{Nx}
 151 values were even higher than those in summer 2010 when the highest summer mean
 152 SAT record was set. T_{Xx} and T_{Nx} were 2.32 and 2.13 °C higher than the 1964–1993
 153 mean and 3.01 and 2.92 standard deviations of the interannual variability (0.77 °C for

154 T_{XX} and $0.73\text{ }^{\circ}\text{C}$ for T_{NX}), respectively. The hot temperature extremes in 2015 also
155 occurred under an increasing trend of temperature extremes. The linear trends are
156 $0.20\text{ }^{\circ}\text{C}/\text{decade}$ for T_{XX} and $0.39\text{ }^{\circ}\text{C}/\text{decade}$ for T_{NX} .

157 The seasonal mean T_{\max} and T_{\min} in summer 2015 showed strong positive
158 anomalies 1.19 and $1.26\text{ }^{\circ}\text{C}$ higher than the 1964–1993 mean. The 2015 T_{\max} anomaly
159 was twice the interannual variability ($0.60\text{ }^{\circ}\text{C}$) and 50% higher than the 2014 anomaly.
160 Western China experienced five more summer days (the annual number of days when
161 $T_{\max} > 25\text{ }^{\circ}\text{C}$) and six more tropical nights (the annual number of days when
162 $T_{\min} > 20\text{ }^{\circ}\text{C}$) in 2015 relative to the 1964–1993 average. The DTR anomaly over
163 western China was negative because the magnitude of the summer mean T_{\min} anomaly
164 was stronger than that of the T_{\max} anomaly. The anomalous negative DTR not only
165 appeared in 2015, but also several times since the mid-1990s, when there was a rapid
166 increase in both the mean temperature and temperature extremes. This indicates that
167 the warming amplitude in T_{\min} is stronger than that in T_{\max} , although they are both in
168 the context of a steady increase.



tion

169

170 Fig. 1. (a, b) Time series of summer 2015 anomalies relative to the climatology (mean of 1964–1993
 171 records) averaged over 165 stations in western China (west of 105° E) using the dataset of
 172 meteorological stations in China. (a) SAT, T_{Xx} and T_{Nx} and (b) T_{max} , T_{min} and DTR. (c–h) Spatial
 173 patterns of 2015 anomalies relative to 1964–1993 for (c) the summer mean SAT, (d) T_{Xx} , (e) T_{Nx} , (f)
 174 T_{max} , (g) T_{min} and (h) DTR from dataset of 165 meteorological stations in western China. Units: °C.

175 The SAT warming signal was observed over a large part of western China (Fig.
 176 1c). The most significant warming was over central and the northern part of western
 177 China, where the anomalies were >3 °C. The maximum anomaly was >11 °C at Yiwu

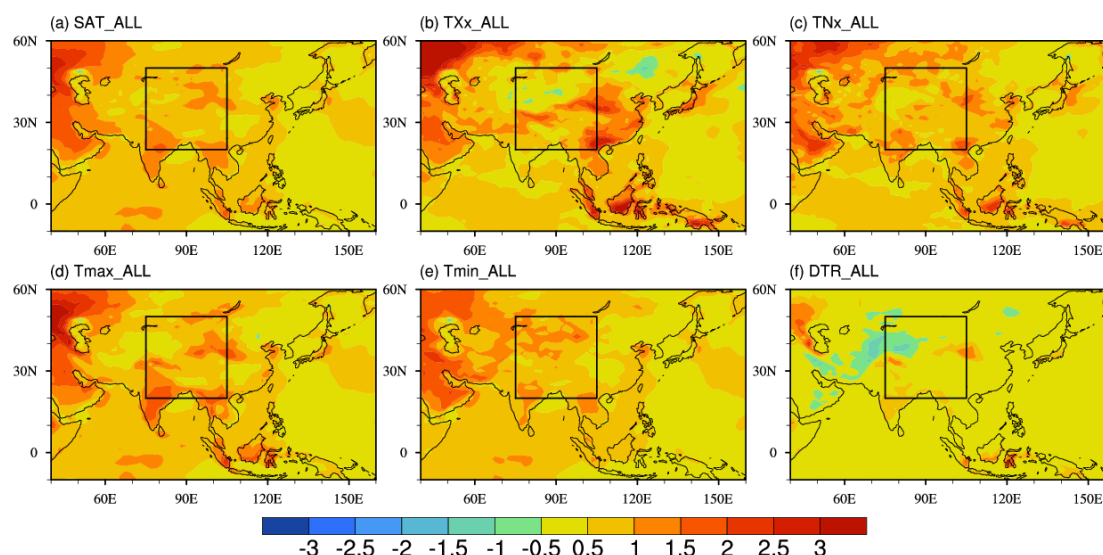
178 station (43.16 °N, 94.42 °E) in Xinjiang province. A remarkable increase in T_{Xx} and
179 T_{Nx} was observed over western China (Fig. 1d and 1e). About 30% (20%) of the
180 stations had a T_{Xx} (T_{Nx}) anomaly >3 °C above the climatology (46 stations for T_{Xx} and
181 36 stations for T_{Nx}). The spatial patterns for the T_{Xx} and T_{Nx} both showed a zonal
182 gradient with a stronger increase in the northern part of western China than in the
183 southern part. This similar distribution implies that regions with a higher hottest
184 daytime temperature generally also had a higher warmest night-time temperature.

185 The seasonal mean T_{max} and T_{min} increased across all of western China (Fig. 1f
186 and 1g). The most significant change for T_{max} was in central western China and the
187 most significant change for T_{min} was in the northwestern part of western China. The
188 magnitude of the T_{min} anomaly was marginally greater than that of the T_{max} anomaly,
189 particularly in the northwest, where the negative DTR anomaly was observed (Fig. 2f).
190 About 50% (88 stations) of the stations had a negative DTR anomaly.

191 **4. Simulated changes in response to different forcings**

192 The model response to changes in the SST/SIE and anthropogenic forcing
193 (2015ALL) relative to the CONTROL experiment reproduced the general patterns of
194 observed SAT warming and the hottest centre in the northern part of western China
195 (Fig. 2a), although the simulated warming signal was more uniform than the observed
196 results. The intensity of the SAT anomaly in response to all changes in forcing was
197 weaker than the anomaly in the observed results, which implies either a deficiency in
198 the model in response to changes in forcing or an effect from the internal variability

199 of atmosphere on the severity of the warming of the SAT in western China in summer
 200 2015.



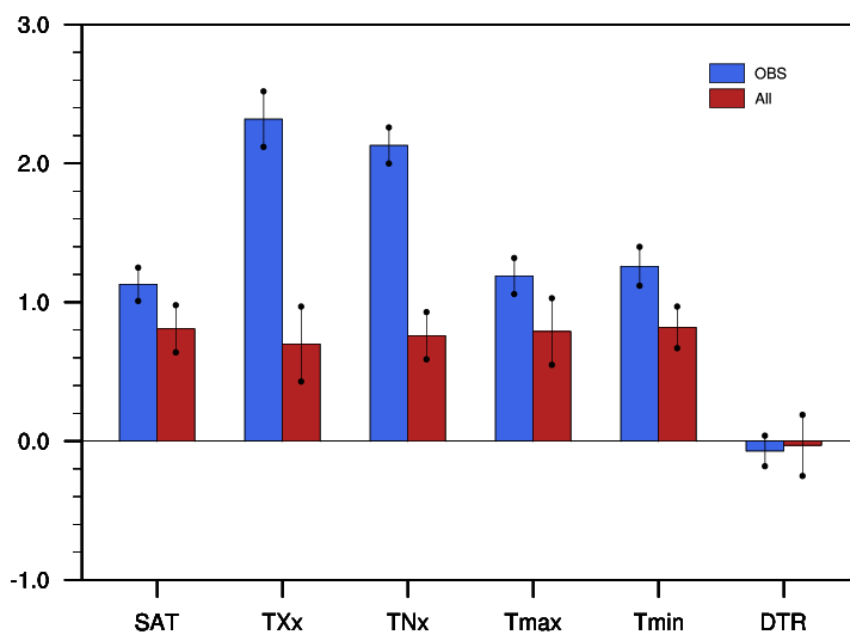
201
 202 Fig. 2. Spatial patterns of changes in (a) the SAT, (b) T_{Xx} , (c) T_{Nx} , (d) T_{max} , (e) T_{min} and (f) DTR in
 203 response to all forcing changes (2015ALL-CONTROL). Units: $^{\circ}C$.

204 T_{Xx} and T_{Nx} in western China increased in response to all forcing changes,
 205 consistent with the observed results (Fig. 2b and 2c). The magnitude of the anomalies
 206 in T_{Xx} and T_{Nx} is underestimated by the simulation, particularly in the north of western
 207 China, but the simulated changes in T_{Xx} and T_{Nx} in south were close to those in the
 208 observations. These results imply a role of changes in the SST/SIE and anthropogenic
 209 forcing in the severity of T_{Xx} and T_{Nx} over western China, particularly over the
 210 southern part of western China.

211 The spatial distribution and intensity of the seasonal mean T_{max} and T_{min}
 212 anomalies were both well simulated by the model in response to all forcing changes
 213 (Fig. 2d and 2e). The negative DTR anomaly in the northwest of western China was

214 also captured by the model. This similarity indicates that changes in the SST/SIE and
215 anthropogenic forcing played a dominant role in the severity of the summer mean
216 T_{\max} and T_{\min} over western China in summer 2015.

217 Figure 3 shows a quantitative comparison of the changes in the mean SAT and
218 temperature extremes over western China in summer 2015 between the observations
219 and the simulated responses. The simulated changes in response to all forcing changes
220 showed a warming SAT and an increase in temperature extremes, although with a
221 weaker magnitude than the observed changes. The area-averaged summer SAT
222 anomaly over western China in response to all forcing changes was 0.81 °C, about 72%
223 of the observed anomaly. The area-averaged T_{\max} and T_{\min} anomalies were 0.79 and
224 0.82 °C, about 66.4 and 65.1% of the observed anomalies, respectively. These results
225 indicate a dominant role of forcing changes, including the SST/SIE and anthropogenic
226 forcing, in the observed summer warming and seasonal mean changes in T_{\max} and T_{\min}
227 over western China in 2015.



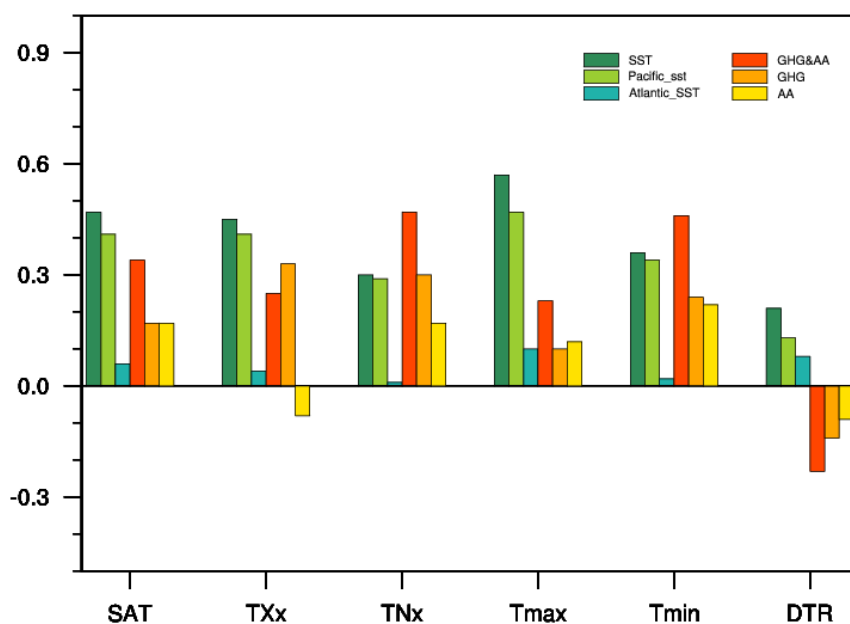
228

229 Fig. 3. Observed and simulated 2015 anomalies for SAT, T_{Xx} , T_{Nx} , T_{max} , T_{min} and DTR over western
 230 China (20–50° N, 75–105° E; masked by the Chinese border) in response to all forcing changes
 231 (2015ALL–CONTROL). The colour bar indicates the central estimates and the dots show the 90%
 232 confidence intervals based on the two-tailed Student's t -test. Units: °C.

233 The magnitude of T_{Xx} and T_{Nx} in the model responses to all forcing changes was
 234 clearly less than that in the observations. The area-averaged T_{Xx} (T_{Nx}) anomalies were
 235 about 30.2% (35.7%) of the observed increase in T_{Xx} (T_{Nx}). The underestimation of
 236 the mean response of the model in the magnitude of these hot temperature extremes
 237 (T_{Xx} and T_{Nx}) indicates the deficiency of the model in response to changes in external
 238 forcing. However, it also implies that the internal variability of the atmosphere might
 239 have played a part in the severity of the hot extremes in western China in 2015. The
 240 role of internal variability of the atmosphere will be discussed later in this paper.

241 Figure 4 shows the relative roles of different forcings in the severity of the
 242 extreme hot event over western China in 2015. The changes in SST/SIE play an

243 important part in the warming of the SAT and the increase in temperature extremes.
 244 The response of the SAT to changes in the SST/SIE is 0.47 °C, explaining 58.0% of
 245 the warming signal in the simulated SAT. For the temperature extremes, the responses
 246 to the changes in the SST/SIE were 0.45 °C for T_{Xx} and 0.57 °C for T_{max} , which were
 247 the most important contributing factors in the simulated increase in T_{Xx} and T_{max} (64.3%
 248 for T_{Xx} and 72.2% for T_{max}). The T_{Nx} and T_{min} response to changes in the SST/SIE
 249 were 0.30 and 0.36 °C, respectively, which represent 39.5 and 43.9% of the simulated
 250 changes. This result indicates that the role of changes in the SST/SIE in the magnitude
 251 of T_{Xx} and T_{max} was stronger than that in T_{Nx} and T_{min} .



252
 253 Fig. 4. Observed and simulated 2015 anomalies for SAT, T_{Xx} , T_{Nx} , T_{max} , T_{min} and DTR over western
 254 China (20–50° N, 75–105° E; masked by the Chinese border) in response to changes in individual
 255 forcings: SST/SIE, 2015SST–CONTROL; Pacific SST, 2015SST–2015SSTATL; Atlantic SST,
 256 2015SSTATL–CONROL; GHG and anthropogenic aerosols (AA), 2015ALL–2015SST; GHG,
 257 2015SSTGHG–2015SST; and AA, 2015ALL–2015SSTGHG. Units: °C.

258 The changes in SST/SIE mainly result from the changes in the SST over the
259 Pacific Ocean, where a super El Niño event was developing in summer 2015.
260 Therefore the increased temperature anomalies in response to the changes in SST/SIE
261 were mainly to the south of 30° N (Supplementary Fig. S1), which were
262 predominantly due to the warming effect related to the El Niño event.

263 The pattern of SST anomalies in summer 2015 suggested a prominent positive
264 SST anomaly over the central and eastern tropical Pacific, which is known as the
265 developing phase of the exceptionally strong 2015–2016 El Niño event
266 (Supplementary Fig. S2a). The El Niño effect warms the tropical and subtropical
267 regions, including the southern part of western China. The warming effect is
268 manifested by a positive atmospheric thickness anomaly (the differences in
269 geopotential height between 200 and 700 hPa) as a Kelvin wave response to strong
270 warming over the central and eastern tropical Pacific (Supplementary Fig. S2b). This
271 positive thickness anomaly corresponds to the anticyclonic circulation anomaly in the
272 lower troposphere over western China (Supplementary Fig. S2c). The anomalous
273 anticyclonic circulation favours an increase in downward solar radiation and warms
274 the air mass by anomalous sinking, therefore contributing to the severity of the hot
275 extremes, particularly the severity of daytime extremes (T_{xx} and T_{max}), over western
276 China.

277 The responses to the direct impacts of changes in GHG and AA forcings explain
278 the remaining magnitude of the simulated SAT warming and increase in temperature

279 extremes (Fig. 4 and Supplementary Fig. S3). Quantitatively, the additional changes
280 of 42.0% in the SAT, 35.7% in T_{XX} , 27.8% in T_{max} , 60.5% in T_{Nx} and 56.1% in T_{min}
281 were responses to the changes in anthropogenic forcing. In general, the effect of
282 changes in GHG concentrations was stronger than that of changes in AA emissions,
283 but they both led to a warming of the SAT and an increase in temperature extremes
284 (except for a decrease in T_{XX} in response to changes in AA forcing). In particular, the
285 responses of temperature extremes to changes in anthropogenic forcing were stronger
286 at night (T_{Nx} and T_{min}) than during the day (T_{XX} and T_{max}). The larger changes in T_{min}
287 than in T_{max} resulted in a negative DTR anomaly in response to forcing by GHG and
288 AA forcing, which was in agreement with the observations, but with a stronger
289 amplitude.

290 The warming induced over western China by AA forcing changes is due to
291 remote changes in the emission of anthropogenic aerosols rather than local changes.
292 Changes in AA emissions in 2015 suggest a reduction over Europe and North America
293 and an increase over South and East Asia (Dong et al., 2016a). The local changes in
294 AA emissions over western China were insignificant. The impacts of a decrease in AA
295 emission over Europe led to local surface warming through aerosol–radiation and
296 aerosol–cloud interactions. This warming extended downwards along the Eurasia
297 continent and induced warming over western China by coupled land
298 surface–atmosphere feedbacks as a result of drying of the land surface and reduced
299 cloud cover, being consistent with the results of Dong et al. (2016b). Thus the surface

300 warming in summer and increases in the temperature extremes over western China
301 were probably the result of the downstream extension of the climate response to
302 reduced AA emissions over Europe (Supplementary Fig. S3).

303 The seasonal mean SAT and temperature extremes over western China for
304 1964–1993 and 2015 in both the observations and 25 realizations in the simulations
305 are shown in Supplementary Fig. S4 to better illustrate the role of the forced response
306 and internal atmospheric variability in the severity of the extreme hot summer of 2015.
307 Basically, CONTROL experiment reproduces the interannual variability of the SAT
308 and temperature extremes over western China in summer. The seasonal mean SAT,
309 T_{N_x} and T_{min} are also in broad agreement with the observations. The biases are the
310 underestimation of T_{max} , T_{Xx} and the DTR, which is a common bias in atmospheric
311 general circulation models (AGCMS; e.g. Kysely and Plavcova, 2012; Cattiaux et al.,
312 2015).

313 The 2015ALL and 2015SST experiments both intensify the seasonal mean SAT
314 and temperature extremes relative to the CONTROL experiment, which suggests that
315 anthropogenic forcing, as well as SST/SIE forcing, affects the severity of surface
316 warming and the increase in temperature extremes in western China. The seasonal
317 mean of T_{Xx} and T_{max} in 2015SST are close to those in 2015ALL, implying a
318 dominant role of the changes in SST/SIE forcing in the simulated response of daytime
319 extremes. The summer mean T_{N_x} and T_{min} in 2015ALL are clearly stronger than those
320 in 2015SST, suggesting that changes in anthropogenic forcing are more effective in

321 increasing the severity of night-time temperature extremes.

322 Interestingly, several realizations in 2015ALL give a magnitude of SAT close to
323 that in summer 2015 in the observations, but no such realization is seen in the
324 CONTROL experiment and the 2015SST simulations (Supplementary Fig. S4a). This
325 suggests that changes in anthropogenic forcing and the SST/SIE set preconditions for
326 the severity of extremely hot SATs over western China, such as summer 2015, to
327 occur in the model simulation. Several realizations in 2015ALL give magnitudes of
328 the SAT and T_{\min} as strong as that in the summer 2015 observations (Supplementary
329 Fig. S4a and S4e). One particular realization with the warmest T_{\min} and the second
330 hottest SAT reproduces the severity of the extremely hot summer of 2015 over
331 western China (Supplementary Figs S5 and S6). In this realization, the magnitude and
332 spatial pattern of the SAT and temperature extremes were similar to those in the
333 summer 2015 observations, suggesting a role for the internal variability of the
334 atmosphere in the severity of the hot extremes over western China in summer 2015.

335 **5. Discussion and conclusions**

336 This study assessed the extent to which the severity of the extreme hot summer in
337 western China in 2015 was forced by changes in the SST/SIE and forcings in GHG
338 and AA emissions and quantified the relative role of individual forcing factors. The
339 main findings can be summarized as follows.

340 1) Observations from meteorological stations in China indicate an extreme hot
341 summer over western China in 2015 (165 stations west of 105 °E). The area-averaged

342 SAT anomaly was 1.13 °C above the 1964–1993 mean, twice the interannual
343 variability. The temperature extremes set the highest records in T_{XX} and T_{Nx} during
344 summer 2015 and were about three times the interannual variability. The extreme hot
345 summer in 2015 occurred in the context of steadily increasing temperatures in recent
346 decades.

347 2) It is estimated that about 65–72% of the observed area-averaged summer
348 mean changes in the SAT, T_{max} and T_{min} over western China in 2015 resulted from
349 changes in boundary forcings, including the SST/SIE and anthropogenic forcing. The
350 magnitude of the area-averaged T_{XX} and T_{Nx} in the model responses to changes in all
351 forcings is about 30.2% (35.7%) of the observed increase in T_{XX} (T_{Nx}). The model
352 results indicate that the internal variability of the atmosphere might play a part in the
353 severity of the observed seasonal mean changes in the SAT, T_{max} , T_{min} and hot
354 temperature extremes over western China in 2015.

355 3) The changes in anthropogenic forcing resulted in about 42% of the simulated
356 warming of the SAT, about 40% of the increase in simulated daytime temperature
357 extremes (T_{XX} and T_{max}) and about 60% of the increase in the simulated night-time
358 temperature extremes (T_{Nx} and T_{min}), suggesting an important role for recent changes
359 in anthropogenic forcing in the severity of hot extremes in western China, particularly
360 night-time extremes. In general, the emissions of GHG and AA both make a positive
361 contribution to the warming of SATs and increases in temperature extremes, although
362 the effects of changes in forcing by GHG are stronger. The increase in the summer

363 mean SAT and temperature extremes in response to changes in AA emissions are
364 probably the result of the downstream extension of the climate response to reduced
365 emissions of AA over Europe.

366 4) The changes in the SST/SIE explain the additional signals in the simulation.
367 The SST changes over the Pacific Ocean, where a super El Niño event was
368 developing, had a dominant role in the response to changes in the SST/SIE. The
369 strong warm SST over the central and eastern tropical Pacific Ocean led to positive
370 anomalies in atmospheric thickness around the tropical and subtropical regions,
371 including the southern part of western China, as a Kelvin wave response. The positive
372 thickness anomalies were related to an anticyclonic circulation anomaly, which
373 favoured an increase in downward solar radiation and therefore contributed to the
374 severity of the hot extremes, particularly to the severity of the daytime extremes (T_{XX}
375 and T_{max}).

376 The simulations indicate that the severity of the extreme hot summer over
377 western China in 2015 was caused by a combination of forced responses and the
378 internal variability of the atmosphere. In addition to tropical forcing, the extreme high
379 temperatures over western China in 2015 were related to a Rossby wave pattern over
380 mid-latitudes extending from the North Atlantic to East Asia. This mid-latitude wave
381 pattern, probably caused by the internal variability of the atmosphere (e.g., Sato et al.
382 2003, 2006; Kosaka et al. 2009), resulted in an anticyclonic circulation over western
383 China that warmed the surface through increased downward solar radiation and the

384 anomalous sinking of an air mass. Thus the observed warming and increase in hot
385 extremes that is not explained by all forcing changes may result from the internal
386 variability of the atmosphere, principally through the mid-latitude Rossby wave
387 pattern.

388 This study detected the forcing response in the severity of SAT warming and
389 increase in temperature extremes over western China in summer 2015. In addition to
390 the changes in the SST/SIE, the changes in anthropogenic forcing set the conditions
391 for the severity of the extreme hot summer in western China in 2015. It should be
392 noted that this study focused on understanding the severity of the extreme hot event
393 over western China in 2015. It differs from previous attribution studies focusing on
394 the risk of occurrence of this event (Miao et al., 2016; Sun et al., 2016). Our results
395 suggest a role for anthropogenic forcing in the severity of this event, while previous
396 studies have argued that the increase in the risk of this kind of hot event can be
397 attributed to human influences. Different aspects of the attribution of the 2015
398 extreme hot event are addressed in our study. Our conclusions are based on the study
399 of one model and the quantitative partitioning of causes could be potentially sensitive
400 to model bias. However, we are confident that our main results are realistic given the
401 model's ability to reproduce the magnitude and spatial characteristics of this extreme
402 temperature event.

403 **Acknowledgements.** This study was supported by the National Natural Science
404 Foundation of China under Grants 416750788, U1502233, 41320104007, by the

405 Youth Innovation Promotion Association of the Chinese Academy of Sciences (No.
406 2018102) and by the UK–China Research & Innovation Partnership Fund through the
407 Met Office Climate Science for Service Partnership China as part of the Newton Fund.
408 BD was supported by the Natural Environment Research Council via the National
409 Centre for Atmospheric Science. The authors thank the two anonymous reviewers for
410 their constructive comments and suggestions on the earlier version of this paper.

411 **References**

- 412 Bindoff, N. L., et al., 2013: *Detection and attribution of climate change: from global*
413 *to regional*. The physical science basis Contribution of working group I to the
414 fifth assessment report of the intergovernmental panel on climate change,
415 Stocker, T. F., et al., Eds., Cambridge University Press, Cambridge,
416 UK,867–952.
- 417 CMA, 2016: *China Climate Bulletin 2015*. China Meteorological Administration, 50
418 pp. (in Chinese)
- 419 Cattiaux, J., H. Douville, R. Schoetter, S. Parey, and P. Yiou, 2015: Projected increase
420 in diurnal and interdiurnal variations of European summer temperatures.
421 *Geophys. Res. Lett.*, **42**, 899–907.
- 422 Christidis, N., P. A. Stott, and S. J. Brown, 2011: The role of human activity in the
423 recent warming of extremely warm daytime temperatures. *J. Climate*, **24**,
424 1922–1930.
- 425 D áz, J., R. Garc á, F. V. de Castro, E. Hernandez, C. Lopez, and A. Otero, 2002:
426 Effects of extremely hot days on people older than 65 years in Seville (Spain)
427 from 1986 to 1997. *Int. of Biometeorol.*, **46**, 145–149.
- 428 Dole, R., et al., 2011: Was there a basis for anticipating the 2010 Russian heat wave?
429 *Geophys. Res. Lett.*, **38**, L06702.
- 430 Dong, B. -W., R. T. Sutton, L. Shaffrey, L. Wilcox, 2016a: The 2015 European heat
431 wave. *Bull. Amer. Meteorol. Soc.*, **97**, S5–S10, doi:

- 432 10.1175/BAMS-D-16-0140.1.
- 433 Dong, B.-W., R. T. Sutton, W. Chen, X. D. Liu, R. Y. Lu, and Y. Sun. 2016b: Abrupt
 434 summer warming and changes in temperature extremes over Northeast Asia
 435 since the mid-1990s: Drivers and physical processes. *Adv. Atmos. Sci.*, **33**,
 436 1005–1023, doi: 10.1007/s00376-016-5247-3.
- 437 Hewitt, H. T., D. Copsey, I. D. Culverwell, et al., 2011: Design and implementation of
 438 the infrastructure of HadGEM3: The next-generation Met Office climate
 439 modelling system. *Geoscientific Model Development*, **4**, 223–253,
 440 doi:10.5194/gmd-4-223-2011.
- 441 Kilbourne, E. M., 1997: Heat Waves and Hot Environments. In *The Public Health
 442 Consequences of Disasters*. In: Noji E K, eds. New York: Oxford University
 443 Press. pp245–269.
- 444 King, A. D, G. J. van Oldenborgh, D. J. Karoly, et al., 2015: Attribution of the record
 445 high Central England temperature of 2014 to anthropogenic influences. *Environ.
 446 Res. Lett.*, **10**, 054002.
- 447 King, A. D., M .T. Black, S. -K. Min, et al., 2016: Emergence of heat extremes
 448 attributable to anthropogenic influences. *Geophys. Res. Lett.*,
 449 doi:10.1002/2015GL067448.
- 450 Kosaka, Y., H. Nakamura, M. Watanabe, and M. Kimoto, 2009: Analysis on the
 451 dynamics of a wave-like teleconnection pattern along the summertime Asian jet
 452 based on a reanalysis dataset and climate model simulations. *J. Meteor. Soc.*

- 453 *Japan*, **87**, 561–580, doi:10.2151/jmsj.87.561.
- 454 Kysely, J., and E. Plavcova, 2012: Biases in the diurnal temperature range in Central
 455 Europe in an ensemble of regional climate models and their possible causes.
 456 *Climate Dyn.*, **39**, 1275–1286.
- 457 Lamarque, J. F., et al., 2010: Historical (1850–2000) gridded anthropogenic and
 458 biomass burning emissions of reactive gases and aerosols: Methodology and
 459 application. *Atmos. Chem. Phys.*, **10**, 7017–7039.
- 460 Lamarque, J. F., et al., 2011: Global and regional evolution of short-lived
 461 radiatively-active gases and aerosols in the Representative Concentration
 462 Pathways. *Climatic Change*, **109**, 191–212.
- 463 Ma, S. M., T. J. Zhou, D. Stone D, et al., 2017: Attribution of the July-August 2013
 464 Heat Event in Central and Eastern China to Anthropogenic Greenhouse Gas
 465 Emissions. *Environ. Res. Lett.*, **12**, 054020.
- 466 Miao, C., Q. Sun, D. Kong, and Q. Duan, 2016: Record-Breaking Heat in Northwest
 467 China in July 2015: Analysis of the Severity and Underlying Causes. *Bull. Amer.*
 468 *Meteor. Soc.*, **97**, S97–S101.
- 469 Otto, F. E. L., et al., 2012: Reconciling two approaches to attribution of the 2010
 470 Russian heat wave. *Geophys. Res. Lett.*, **39**, L04702.
- 471 Rahmstorf, S., and D. Coumou, et al., 2011: Increase of extreme events in a warming
 472 world. *Proc. Natl. Acad. Sci.*, **108**, 17905–17909.
- 473 Rayner, N. A., et al., 2003: Global analyses of sea surface temperature, sea ice, and

- 474 night marine air temperature since the late nineteenth century. *J. Geophys. Res.*,
- 475 **108**, 4407
- 476 Sato, N., and M. Takahashi, 2003: Formation mechanism of vorticity anomalies on the
- 477 subtropical jet in the midsummer northern hemisphere. *Theoretical and Applied*
- 478 *Mechanics Japan*, **52**, 109–115, doi:10.11345/nctam.52.109.
- 479 Sato, N., and M. Takahashi, 2006: Dynamical processes related to the appearance of
- 480 quasi-stationary waves on the subtropical jet in the midsummer northern
- 481 hemisphere. *J. Climate*, **19**, 1531–1544, doi:10.1175/JCLI3697.1.
- 482 Seneviratne, S. I., et al., 2012: Changes in climate extremes and their impacts on the
- 483 natural physical environment. In: Field CB et al., eds. Managing the risks of
- 484 extreme events and disasters to advance climate change adaptation. A special
- 485 report of working groups I and II of the IPCC. Cambridge: Cambridge
- 486 University Press.
- 487 Stott, P. A., et al., 2013: Attribution of Weather and Climate-Related Events. In: Asrar
- 488 G, Hurrell J, eds. Climate Science for Serving Society.
- 489 Stott, P. A., 2016: How climate change affects extreme weather events. *Science*, **352**,
- 490 1517–1518.
- 491 Sun, Y., L. C. Song, H. Yin, et al., 2016: Human Influence on the 2015 extreme high
- 492 temperature events in western China. *Bull. Amer. Meteorol. Soc.*, **97**, S5–S9.
- 493 WMO, 2015: The state of greenhouse gases in the atmosphere based on global
- 494 observations through 2014. WMO Greenhouse Gas Bull. No. 11 4 pp.

- 495 WMO Press Conference, 2015: Status of the global climate in 2015 Geneva, 25
496 November 2015. [Available online at
497 [http://webtv.un.org/meetings-events/watch/wmo-press-conference-status-of-the-
498 global-climate-in-2015-geneva-25-november-2015/4631098881001#full-text](http://webtv.un.org/meetings-events/watch/wmo-press-conference-status-of-the-
498 global-climate-in-2015-geneva-25-november-2015/4631098881001#full-text)].
499 [Accessing data: November 25, 2015].
- 500 Xinhua net, 2015. Feel the “fire Island” Turpan extreme high temperature 24 July
501 2015. [Available online at
502 http://news.xinhuanet.com/politics/2015-07/24/c_128057198.html]. [Accessing
503 data: July 24, 2015].
- 504 Zwiers, F. W., X. B. Zhang, and Y. Feng, 2011: Anthropogenic influence on long
505 return period daily temperature extremes at regional scales. *J. Climate*, **24**,
506 296–307
- 507 Zhou, B. T., Y. Xu, J. Wu, S.Y. Dong, and Y. Shi, 2016: Changes in temperature and
508 precipitation extreme indices over China: analysis of a high-resolution grid
509 dataset. *Int. J. Climatol.*, **36**, 1051–1066.